REVISION 1

Darrellhenryite, $Na(LiAl_2)Al_6(BO_3)_3Si_6O_{18}(OH)_3O$, a new mineral from the tourmaline supergroup

Milan Novák[1*], Andreas Ertl[2], Pavel Povondra[3], Michaela Vašinová Galiová[4,5], George R. Rossman[6], Helmut Pristacz[2], Markus Prem[2], Gerald Giester[2], Petr Gadas[1] and Radek Škoda[1]

[1]Department of Geological Sciences, Masaryk University, Kotlářská 2, 611 37, Brno, Czech Republic
[2]Institut für Mineralogie und Kristallographie, Geozentrum, Universität Wien, Althanstrasse 14, 1090 Wien, Austria
[3]Department of Geochemistry, Mineralogy and Natural Resources, Charles University, Albertov 6, 128 43 Praha 2, Czech Republic
[4]Department of Chemistry, Masaryk University, Kotlářská 2, 611 37 Brno, Czech Republic
[5]Central European Institute of Technology (CEITEC), Masaryk University, Kamenice 5, 625 00 Brno, Czech Republic
[6]Division of Geological and Planetary Sciences, California Institute of Technology, Pasadena, CA 91125-2500, USA

*E-mail: mnovak@sci.muni.cz

ABSTRACT

Darrellhenryite, $Na(LiAl_2)Al_6(BO_3)_3Si_6O_{18}(OH)_3O$, a new member of the tourmaline supergroup (related to the alkali-subgroup 4), is a new Li-bearing tourmaline species, which is closely related to elbaite through the substitution ${}^{Y}Al_{0.5}{}^{W}O_1\ {}^{Y}Li_{-0.5}{}^{W}(OH)_{-1}$. It occurs in a complex (Li-bearing) petalite-subtype pegmatite with common *lepidolite*, Li-bearing tourmalines, and amblygonite at Nová Ves near Český Krumlov, southern Bohemia, Moldanubian Zone, Czech Republic. This pegmatite dike is zoned cross-cuts a serpentinite body enclosed in leucocratic granulites. Pink darrellhenryite forms columnar crystals (sometimes in parallel arrangement) up to 3 cm long and up 2 cm thick, associated with albite (var. *cleavelandite*), minor quartz, K-feldspar, petalite, rare polylithionite and locally rare

pollucite. The optical properties and the single-crystal structure study ($R1 = 0.019$) of darrellhenryite are consistent with trigonal symmetry, $\omega = 1.636(2)$, $\varepsilon = 1.619(2)$, birefringence: 0.017, space group $R3m$, $a = 15.809(2)$, $c = 7.089(1)$ Å, $V = 1534.4(4)$ Å^3, and $Z = 3$. The chemical analysis, in combination with the results from the single-crystal structure refinement, gives the formula $^{X}(Na_{0.58}Ca_{0.01}\square_{0.41})_{1.00}\ ^{Y}(Li_{1.05}Al_{1.95})_{3.00}\ ^{Z}Al_6\ (BO_3)_3\ ^{T}(Si_6O_{18})\ ^{V}(OH)_3\ ^{W}(O_{0.66}F_{0.34})_{1.00}$, which can be simplified to an ideal formula of $Na(LiAl_2)Al_6(BO_3)_3Si_6O_{18}(OH)_3O$. The strongest lines of the powder pattern [d in Å (I, hkl)] are 4.180 (39, 211), 3.952 (54, 220), 3.431 (73, 012), 2.925 (100, 122), 2.555 (90, 051), 2.326 (42, 511), 2.029 (42, 223), 2.021 (42, 152), 1.901 (50, 342), 1.643 (49, 603). The density is $D_{meas} = 3.03(3)$ g/cm^3, $D_{calc} = 3.038$ g/cm^3. Darrellhenryite is considered to have crystallized in Li- and B-rich but F-moderate environments in complex pegmatites; no influence of higher activity of O on the darrellhenryite formation is implied from its mineral assemblage. The name is for Darrell J. Henry, Professor of Geology at the Louisiana State University, Baton Rouge, USA, an expert on the mineralogy, petrology, crystal chemistry and nomenclature of tourmaline-supergroup minerals.

Key words: Darrellhenryite, tourmaline group, chemical analyses, crystal structure, Nová Ves, Czech Republic

INTRODUCTION

Lithium-bearing tourmalines are of considerable scientific interest because they reflect compositional trends in granitic pegmatites (e.g., Selway et al. 1999, 2002), because of their complex zoning (e.g., Lussier et al. 2011) and because of their unknown stability field (e.g., London 2011). The current nomenclature of the tourmaline supergroup includes eight Li-bearing tourmalines (Henry et al. 2011), four of which are known to exist in nature: elbaite (Vernadsky 1913), fluor-liddicoatite (Dunn et al. 1977), rossmanite (Selway et al. 1998), and fluor-elbaite (Bosi et al. 2013) and four hypothetical species (Table 1). Darrellhenryite, $Na(LiAl_2)Al_6(BO_3)_3Si_6O_{18}(OH)_3O$, represents a new Li-bearing tourmaline species which belongs to the oxy-tourmaline series as do povondraite and chromo-alumino-povondraite (Henry et al. 2011) and the more recently described minerals - oxy-schorl (Bačík et al. 2013) and oxy-dravite (Bosi and Skogby 2012). In this contribution, we present chemical analyses,

the description of the crystal structure, spectroscopic data and discuss paragenetic position of darrellhenryite in complex granitic pegmatites.

Darrellhenryite has been approved by the IMA-CNMNC (proposal no. 2012-026). Its chemical composition relates to the alkali-subgroup 4 (Table 1; Henry et al. 2011), which requires a new root name in this case, the name chosen is *darrellhenryite*, in honor of Darrell J. Henry (born 1953), Professor of Geology at the Louisiana State University, Baton Rouge, USA, an expert on the mineralogy, petrology, crystal chemistry and nomenclature of tourmaline-supergroup minerals. The type specimen is deposited with the Department of Mineralogy and Petrography of the Moravian Museum, Zelný trh 6, 659 37 Brno, Czech Republic, catalogue number B10661. Holotype material (the crystal chosen for structure refinement) is deposited at the Smithsonian Institution, National Museum of Natural History, Washington D.C., catalogue number NMNH 175992, and co-type material is also deposited at this museum, catalogue number NMNH 175993.

OCCURRENCE

Darrellhenryite was discovered in a complex (Li-bearing) pegmatite at Nová Ves near Český Krumlov, southern Bohemia, Czech Republic. The pegmatite belongs to the Moldanubian pegmatite province along with about 100 other lepidolite- and elbaite-subtype pegmatite bodies of the Variscan age (Novák and Povondra 1995; Novák 2005; Breiter et al. 2010; Ertl et al. 2004, 2012; Melleton et al. 2012). The pegmatite occurs as a symmetrically zoned dyke, up to 8 m thick and about 100 m long, that cuts a serpentinite body (Teertstra et al. 1995; Novák and Černý 1998), which is enclosed in leucocratic granulites of the Blanský les Massif. From the contact inwards, it consists of: (i) an outermost granitic unit with biotite, (ii) a coarse-grained albite unit locally with graphic intergrowths of Kfs + Qtz and aggregates of Ms + Qtz + Tur; (iii) blocky K-feldspar and blocky petalite, and (iv) an albite-lepidolite unit, the latter three units also containing Li-bearing tourmalines. No pockets have been found in the pegmatite. The Li-bearing primary minerals in the pegmatite are: petalite > *lepidolite* (trilithionite > polylithionite) > Li-bearing tourmalines (darrellhenryite > fluor-elbaite) > amblygonite. Secondary spodumene + quartz aggregates after petalite and secondary montebrasite after primary amblygonite are also present. Accessory almandine-spessartine, fluorapatite, beryl, zircon, pollucite, cassiterite, columbite, and microlite-group minerals (fluornatromicrolite to fluorcalciomicrolite) were also found in the pegmatite. The pegmatite

may be classified as a complex(Li)-type, petalite-subtype following the scheme proposed by Černý and Ercit (2005) but with substantial amounts of *lepidolite*, Li-bearing tourmalines and amblygonite. The mineral assemblage and modal proportion of Li-bearing minerals are similar to much larger pegmatites of the petalite-subtype (e.g., Tanco, SE Manitoba, Canada; Stilling et al. 2006, and Utö, Stockholm region, Sweden; Smeds and Černý 1989; Selway et al. 2002); however, the overall amount of Li-bearing minerals is much lower in the Nová Ves pegmatite than in these pegmatites.

Darrellhenryite (holotype) forms subhedral, short, columnar crystals and parallel aggregates, up to 3 cm long and up 2 cm thick, which occur exclusively in the *cleavelandite*-rich portions of the albite-lepidolite unit in the central part of the dyke. The associated minerals also include minor quartz, relics of pale brown, blocky K-feldspar and colorless blocky petalite, rare colorless flakes of polylithionite and locally rare altered pollucite. Very rare inclusions of late muscovite, visible only in BSE images, occur within the aggregates of darrellhenryite.

METHODS

Chemical composition

Chemical analyses of darrellhenryite were carried out by a variety of methods. These included a complete wet chemical analysis (Povondra et al. 1985); 13 EMP analyses (using WDS) with a Cameca SX 100 electron microprobe, LA-ICP-MS (Li; 8 analyses); and a combination of wet chemical, near-IR, and thermogravimetric analysis (TGA; 3 analyses) for H_2O. To determine the OH content of darrellhenryite, ~15 mg of the material was used for each analysis, performed on a Mettler-Toledo TGA/SDTA 851 (University of Vienna). The powder was heated from 25 to 1100 °C (5 °C/min) in N_2 gas (gas flow: 25 mL/min). Analytical data of darrellhenryite, including standards for EMPA, are given in Table 2. A synthetic multi-layered pseudocrystal (Si/W layers, d = 60 Å, PC1 in terms of Cameca) was used as reflector for the fluorine analysis. It provides a much higher count rate than the more commonly used TAP (thalium acid phtalate) crystal. The substantial overlap of the FK_α position with the shoulder of the Fe$L_{\alpha,\beta}$ peak on the pseudocrystal (Witter and Kuehner 2004) is not significant due to very low Fe content in darrellhenryite. The PHA settings of the detector were used in differential mode (baseline 750 mV and window 3500 mV) to reduce the "Bremsstrahlung" intensity and the influence of the 2nd order of the AlK_α peak on the low

129 background position. We chose a natural *lepidolite* with well defined F content (8.45 wt.% F)
130 as a standard. Prior to conducting the analysis, care was taken to determination precise
131 background positions and the peak maximum of the FK_α line. The positions of the FK_α peak in
132 darrellhenryite and *lepidolite* are identical. The fluorine peak counting time was 60 s and 30 s
133 on each of the background positions, and the exponential fit of background was used. Raw
134 EMPA data and B, H and Li content determined by Povondra et al. (1985), were corrected
135 using the X-Phi (Merlet 1994) matrix procedure.
136 Concentration of Li and trace elements and were investigated by LA-ICP-MS
137 (Department Chemistry, Masaryk University, Brno) using an Agilent 7500ce (Agilent
138 Technologies, Santa Clara, CA, USA) quadrupole ICP-MS with an attached UP 213 laser
139 ablation system (New Wave Research, Inc., Fremont, CA, USA). The samples were placed
140 into a SuperCell (New Wave Research, Inc., Fremont, CA, USA) having volume of 33 cm^3
141 and ablated using a commercial Q-switched Nd:YAG laser operated at a wavelength of 213
142 nm (pulse duration 4.2 ns). Ablated material was transported from the sample chamber using
143 helium carrier gas (1 $l.min^{-1}$) and mixed with argon (0.6 $l.min^{-1}$) prior to the torch.
144 Optimization of LA-ICP-MS parameters (gas flow rates, sampling depth, voltage of ion
145 optics) was performed using glass reference material NIST SRM 612 to maximize the S/N
146 ratio. Potential polyatomic interferences were minimized by a collision reaction cell in He
147 mode (2.5 $ml.min^{-1}$).

148 **Crystal Structure**

149 The tourmaline of darrellheryite was studied on a Bruker AXS Kappa APEX II CCD
150 diffractometer equipped with a monocapillary optics collimator and graphite-
151 monochromatized Mo$K\alpha$ radiation. Single-crystal X-ray diffraction data were collected at
152 room temperature (out to ~80° 2θ), integrated and corrected for Lorentz and polarization
153 factors and absorption correction by evaluation of partial multiscans. The structure was
154 refined (using a starting model; Ertl et al. 2010) with SHELXL-97 (Sheldrick 1997) using
155 scattering factors for neutral atoms. The H atom bonded to the O3 atom was located from a
156 difference-Fourier map and subsequently refined. Refinement was performed with anisotropic
157 displacement parameters for all non-hydrogen atoms. Table 3 provides crystal data and details
158 of the structure refinement. Site occupancies were refined according to well-known
159 characteristics of the tourmaline structure (B, O1-O8, and H3 were constrained to fully
160 occupy their respective sites, Na was refined at the *X* site, Al and Li were refined at the *Y* site;

for other details see Table 4). The refinements converged at $R1(F)$ values of ~1.95% (Table 3). The atomic parameters and equivalent isotropic displacement parameters are given in Table 4. In Table 5 we present selected interatomic distances.

The X-ray powder diffraction (XRD) data for darrellhenryite (pinkish white powder) were collected on a PW 3710 Philips diffractometer using Cu$K\alpha$ radiation (40 kV, 40 mA), equipped with a secondary graphite monochromator. The irradiated sample area was constantly 12 x 12 mm^2 (automatic divergence slits gave a constant area for each 2θ angle). A sample of darrellhenryite was prepared on a round zero-background silicon holder, dispersed in a few drops of acetone and allowed to dry. The XRD data were collected (at 295(1)K) over the 2θ range of 5-62 ° using 0.01 ° steps and a counting time of 1 sec/step. Because of the very limited amount of material with a composition close to the endmember of darrellhenryite, the collection of high-quality data was limited to 2θ less than 65 ° because of the low quality of data at higher angles. Silicon SRM 640b was used as internal standard. The powder diffraction data (indexing is based on the structure refinement and only reflections with $I_{calc} \geq 1$ are listed) are listed in Table 6.

Spectroscopic Investigations

Near-infrared spectra were obtained with a Nicolet Magna 860 FTIR, a silica beam splitter, and a tungsten-halogen source. Polarized spectra were obtained with a $LiIO_3$ crystal polarizer. The darrellhenryite sample was prepared as a doubly-polished 1.132 mm thick slab, in which the c axis is parallel to the section plane. A small, clear area was located in the otherwise cracked sample through which the spectrum could be obtained. The OH content was determined from the integrated area of the OH overtone bands in the 6350 to 7300 cm^{-1} region. Because a calibration of this method specific to this species does not exist, the calibration used in Ertl et al. (2010) for elbaite-schorl series tourmalines was chosen for this study. Optical spectra in the visible to near-infrared region were obtained with a home-built microspectrometer based on diode-array technology, as described in Taran and Rossman (2001).

RESULTS

Physical and optical properties

Darrellhenryite has vitreous luster and a pinkish white streak. The crystals are translucent to transparent with an intense to pale pink color. The mineral is brittle with conchoidal fracture. Mohs hardness is ~ 7. The measured density reported by Povondra et al. (1985) is 3.03(3) g cm^{-3}. The calculated density is 3.041 g cm^{-3} using the empirical formula given by Povondra et al. (1985) and the present unit cell (single-crystal) data whereas the calculated density is 3.038 g cm^{-3} using the present empirical formula and unit cell data (single-crystal data). Darrellhenryite is non-fluorescent under long, medium or short-wave UV light. It is uniaxial (-), ω = 1.636(2), (1.637) ε = 1.619(2), (1.621) (590 nm); birefringence: 0.017 (0.016) (data in parentheses - Povondra et al. 1985). In thin section, it is colorless. Fragments about 1 cm thick show pleochroism that varies from near colorless (\\c) to pale pink ($\perp$c).

The color is caused primarily by an absorption band centered at ~520 nm in the polarization direction perpendicular to c (Fig. 1). Weak, sharper features occur at 449 and 457 nm, and a hint of a broad and weak band appears centered at ~700 nm. All of these features and the band in the E\\c direction are characteristic of most pink tourmalines, which owe their color to Mn^{3+} believed to be produced by the natural irradiation of Mn^{2+} in the tourmaline (Reinitz and Rossman 1988). The sample is full of pervasive internal fractures, which cause the wave-like appearance in the spectrum (Fig. 1) due to interference fringes. A 10.4 μm thick air gap in this particular sample would produce the fringes seen in Figure 1. Spectra obtained from different areas in the sample had significant differences in the intensity of the 520 nm band, attributed to Mn, indicating an inhomogeneous distribution of this chromophore.

Chemical composition

The empirical formulas are calculated on the basis 31 (O,OH,F): $(Na_{0.55}K_{0.02}Ca_{0.01}\square_{0.42})_{\Sigma 1.00}\,(Li_{1.19}Fe_{0.02}Al_{1.96})_{\Sigma 3.17}\,Al_{6.00}\,(BO_3)_{3.00}\,(Si_{5.99}Al_{0.01})O_{18}\,(OH)_{3.00}(O_{0.67}F_{0.32}OH_{0.01})$ – (Povondra et al. 1985) and $(Na_{0.58}Ca_{0.01}\square_{0.41})_{\Sigma 1.00}\,(Li_{1.03}Al_{2.02})_{\Sigma 3.05}\,Al_{6.00}\,(BO_3)_{2.98}\,Si_{6.01}O_{18}\,(OH)_{3.00}(O_{0.65}F_{0.35})$ – a combination of EMPA, LA-ICP-MS (Li), TGA (H_2O), and B_2O_3 taken from Povondra et al. (1985). The ideal formula for darrellhenryite is: $Na_{1.00}\,(Li_{1.00}Al_{2.00})_{\Sigma 3.00}\,Al_{6.00}\,(BO_3)_{3.00}\,Si_{6.00}\,O_{18}\,(OH)_{3.00}\,O_{1.00}$. Very low concentrations of other elements (Fe, Mn, K, Ca) are typical, as well as moderate contents of F (Table 2). Analyses obtained using LA-ICP-MS indicate that most trace elements are present at or below the detection limits (0.1-15 ppm) except for low contents (+ detection

limits in parentheses) of Be (≤ 17; 0.1), Ni (≤ 11; 0.3), Cu (≤ 13; 1), Zn (≤ 10; 3) and Sn (≤ 77; 2) (all in ppm) and high contents of Ga (134-405 ppm; 2). The Ga content is comparable to that of Cu-enriched Li-bearing tourmalines from pegmatites in Brazil, Nigeria and Mozambique (Perretti et al. 2010), but higher than that of black tourmaline from NYF-type pegmatites of the Třebíč Pluton, Czech Republic, with Ga = 78-160 ppm (Novák et al. 2011), and black tourmaline from common pegmatites of the Strážek Moldanubicum, Czech Republic, with Ga = 2-212 ppm (Gadas et al. 2012).

Near-IR Spectrum

Water content can be determined from the intensity of the OH overtone absorptions in the 7000 cm^{-1} region of the near-infrared spectrum (Fig. 2). The total integrated area of the spectrum (\\c + 2×⊥c) in Figure 2 is 1092.5 per cm^2 (normalized to 1 cm thickness). Using the density of 3.038 gcm^{-3} and dividing by the factor 113 (taken from Ertl et al. 2010), an H_2O concentration of 2.87 wt% is determined. This is in remarkably close agreement with the value in Table 2, 2.86 wt%, determined by classical wet chemical methods and with the value determined by thermogravimetric analysis (TGA) [2.9(1) wt%; Table 2]. This value is also consistent with the proposed darrellhenryite formula.

Crystallography

Single-crystal X-ray studies gave the following data: trigonal symmetry, space group: *R*3*m*, *a* = 15.809(2), *c* = 7.089(1) Å, *V* = 1534.4(4) $Å^3$, and *Z* = 3. Darrellhenryite is isotypic with elbaite and other rhombohedral (*R*3*m*) members of the tourmaline supergroup. The refined formula for darrellhenryite, $^{X}(Na_{0.56}\square_{0.44})\ ^{Y}(Li_{1.05}Al_{1.95})_{\Sigma 3.00}\ ^{Z}Al_6\ ^{T}(Si_6O_{18})\ (BO_3)_3\ ^{V}(OH)_3\ ^{W}(O_{0.66}F_{0.34})$, is in reasonably good agreement with the empirical formula $^{X}(Na_{0.58}Ca_{0.01}\square_{0.41})\ ^{Y}(Li_{1.03}Al_{2.02})_{\Sigma 3.05}\ ^{Z}Al_6\ (BO_3)_{2.98}\ ^{T}(Si_6O_{18})\ ^{V}(OH)_3\ ^{W}(O_{0.65}F_{0.35})$; slight differences are within the limits of the refinement and may also reflect minor chemical zoning confirmed by chemical analyses and different ways of formula elucidation.

An H atom (H3) at the site associated with O3 was easily located in this refinement. Ertl et al. (2002) showed that the bond-angle distortion (σ_{oct}^2) of the ZO_6 octahedron in a tourmaline is largely a function of the <*Y*-O> distance of that tourmaline, although the occupant of the O(3) site (*V* position in the general formula) also affects that distortion. The

255 covariance, *r*, of <*Y*-O> and σ_{oct}^2 of the ZO_6 octahedron is -0.99 (Fig. 2 in Ertl et al. 2005) for
256 all investigated tourmalines whose V site is occupied by 3 (OH) groups. Darrellhenryite (with
257 $^{Z}\sigma_{oct}^2 = 52.85$ and <*Y*-O> ≈ 1.984; Table 5) lies exactly on the *V* site = 3 (OH) line. Hence, the
258 *V* site of darrellhenryite is completely occupied by (OH). The refinement shows that the *W*
259 site is occupied by ($O_{0.66}F_{0.34}$) (Table 4, Fig. 3). Hence, this site is clearly dominated by
260 oxygen, considering also the chemical data (Table 2).
261 The *T* site is completely occupied by Si. A refinement of Si ↔ B at the T site gives no
262 clear indication for significant amounts of $^{[4]}$B (>0.10 apfu). Hence, in the final refinement the
263 *T* site was refined only with Si (Table 4). Recently, Lussier et al. (2011) investigated
264 liddicoatite samples from Anjanaboina, Madagascar, which contain essentially no $^{[4]}$B. Most
265 of these Al- and Li-rich tourmalines have a <*T*-O> distance of 1.617(1) Å, which is in good
266 agreement with the <*T*-O> distance of ~1.616(1) Å in darrellhenryite (Table 5).
267 The X-ray powder diffraction data for darrellhenryite is presented in Table 6. The 10
268 reflections with the highest intensity are in bold letters. Unit cell parameters refined from the
269 powder data (Table 6), obtained by a least-squares refinement of the setting angles of all
270 reflections, are as follows: $a = 15.820(2)$, $c = 7.093(1)$ Å, $V = 1537.4(6)$ Å^3, very similar to
271 those from the single-crystal X-ray study and data of Povondra et al. (1985).
272

273 **COMPOSITIONAL EVOLUTION OF TOURMALINES FROM THE NOVÁ VES PEGMATITE AND**
274 **PARAGENETIC POSITION OF DARRELLHENRYITE**

275 Tourmaline is a common accessory mineral in complex pegmatites of the Moldanubian Zone
276 including the Nová Ves pegmatite (Povondra et al. 1985; Novák and Povondra 1995; Novák
277 et al. 2004; Breiter et al. 2010). Its chemical composition evolves during pegmatite
278 crystallization: black Mg-poor oxy-schorl from the outer albite unit → black oxy-schorl to
279 blue or green Fe-rich fluor-elbaite in muscovite + quartz aggregates from the albite unit →
280 green Fe-rich fluor-elbaite to pink fluor-elbaite to darrellhenryite from outer parts of the
281 albite-lepidolite unit → pink to pinkish darrellhenryite in albite (*cleavelandite*) from the inner
282 part of the albite-lepidolite unit (Fig. 3). The compositional trends (behavior of Na, Al, Fe, F)
283 are similar to ordinary lepidolite-subtype pegmatites from the Moldanubian Zone (Selway et
284 al. 1999; Novák 2000); however, most tourmalines from Nová Ves belong to the oxy series
285 (Fig. 3). Based on a large set of EMP analyses, rossmanite, a common accessory mineral in

the lepidolite-subtype pegmatites from the Moldanubian Zone, Czech Republic (Selway et al. 1998, 1999), has not been identified from the Nová Ves locality.

Darrellhenryite is evidently the least common Li-bearing tourmaline, and it is known only from the Nová Ves locality. The mineral assemblage of darrellhenryite (holotype + other samples) is characterized by abundant albite + minor quartz ± K-feldspar ± petalite (or secondary spodumene + quartz) ± rare polylithionite ± pollucite. It differs from other pink Li-bearing tourmalines in complex pegmatites of lepidolite-subtype and elbaite-subtype from the Moldanubian Zone. In lepidolite-subtype pegmatites, pink Li-bearing tourmaline (fluor-elbaite > rossmanite > elbaite; Povondra et al. 1985; Selway et al. 1998, 1999; Novák 2000) is typically associated with common Li-rich micas (trilithionite > polylithionite; Černý et al. 1995) + albite ± quartz, and this assemblage indicates high activity of F. In elbaite-subtype pegmatites, red to pink Li-bearing tourmaline (fluor-elbaite > fluor-liddicoatite; Povondra et al. 1985; Novák et al. 1999a, 2012) is commonly the only Li-bearing mineral, Li-rich micas (polylithionite; Novák and Povondra 1995; Novák et al. 1999b; Zahradníček and Novák 2012) being absent or very rare; hence, F enters almost exclusively tourmaline. Consequently, composition of associated Li-rich micas and their abundance play a crucial role in the formation of darrellhenryite because they control activities of Li and F in the system. Darrellhenryite is likely related to Li- and B-rich but F-moderate environments characterized by the assemblage albite ± quartz > Li-rich micas. No influence of higher activity of O on the darrellhenryite formation is inferred from the mineral assemblage, similar to the case of oxy-schorl (Bačík et al. 2012).

Due to a low number of complete chemical analyses of Li-bearing tourmalines and because we did not find any chemical analysis of Li-bearing tourmaline corresponding to darrellhenryite, we checked also electron microprobe analyses of Ca-poor Li-bearing tourmalines published to date, where Li and H were calculated using stoichiometric constraints: Li (apfu) = 15 - $\sum$ (*Y*+*Z*+*T*) and (OH+F) = 4 (e.g., Selway et al. 1999). Only a few analyses of pink Li-bearing tourmalines show a combination of Na, Al and F contents (Na > 0.5 apfu, Al > 7.5 apfu, F < 0.5 apfu), which are indicative of darrellhenryite. The samples come from Dobrá Voda, Czech Republic (Table 1, anal. No. 9; Selway et al. 1999), Tanco, SE Manitoba, Canada (Table 4, anal. No. 5; Selway et al. 2000), Utö, Sweden (Table 2, anal. No. 7; Selway et al. 2002), and Bennet Mine, southern Maine (Table 8, anal. No. 8; Wise and Brown 2010). They typically show high vacancies at the *X* site (~0.43-0.48 pfu) and low to

318 moderate F (0.23-0.39 apfu), so they are compositionally close to rossmanite (Selway et al.
319 1998). Consequently, a detailed study (ideally including EMPA, single crystal X-ray
320 diffraction, LA-ICP-MS, SIMS, and spectroscopic methods) is required to distinguish the Ca-
321 poor Li-bearing tourmalines - elbaite, fluor-elbaite, rossmanite, darrellhenryite, and the
322 hypothetical □-Li-O phase (Table 1) - vacant subgroup 4 (Henry et al. 2011).
323

324 **Acknowledgements**

325 We sincerely thank the reviewers A. McDonald and F. Colombo for their careful reviews of
326 the manuscript as well as the comments of the members of the CNMNC of the IMA, which
327 improved this manuscript significantly. This work was funded by GAP 210/10/0743 (MN, PG
328 and RŠ) and by the Austrian Science Fund (FWF) project no. P23012-N19 (AE) with
329 contributions from NSF grant EAR-0947956 (GRR). MVG acknowledges the European
330 Regional Development Fund project "CEITEC" (CZ.1.05/1.1.00/02.0068).
331
332

333 **REFERENCES CITED**

334

335 Bačík, P., Cempírek, J., Uher, P., Novák, M., Ozdín, D., Filip, J., Škoda, R., Breiter, K.,
336 Klementová, M., Ďuďa, R., and Groat, L. (2013) Oxy-schorl,
337 $Na(Fe^{2+}_2Al)Al_6Si_6O_{18}(BO_3)_3(OH)_3O$, a new mineral from Zlatá Idka, Slovak Republic and
338 Přibyslavice, Czech Republic. American Mineralogist, 98, 485–492.
339 Bosi, F. and Skogby, H. (2012) Oxy-dravite, IMA 2012-004a. CNMNC Newsletter No. 14,
340 October 2012, page 1285; Mineralogical Magazine, 76, 1281–1288.
341 Bosi, F., Andreozzi, G.B., Skogby, H., Lussier, A.J., Abdu, Y. and Hawthorne, F.C. (2013)
342 Fluor-elbaite, $Na(Li_{1.5}Al_{1.5})Al_6(Si_6O_{18})(BO_3)_3(OH)_3F$, a new mineral species of the
343 tourmaline supergroup. American Mineralogist (in press).
344 Breiter, K., Cempírek, J., Kadlec, T., Novák, M., and Škoda, R. (2010) Granitic pegmatites
345 and mineralogical museums in Czech Republic. Acta Mineralogica et Petrographica, IMA
346 2010 Field Guide Series, 6, 1–56.
347 Černý, P. and Ercit, T.S. (2005) The classification of granitic pegmatites revisited. Canadian
348 Mineralogist, 43, 2005–2026.

Černý, P., Staněk, J., Novák, M., Baastgaard, H., Rieder, M., Ottolini, L., Kavalová, M., and Chapman, R. (1995) Chemical and structural evolution of micas at the Rožná and Dobrá Voda pegmatites, Czech Republic. Mineralogy and Petrology, 55, 177–202.

Dunn, P.J., Appleman, D.E., and Nelen, J.E. (1977) Liddicoatite, a new calcium end-member of the tourmaline group. American Mineralogist, 62, 1121–1124.

Ertl, A., Hughes, J.M., Pertlik, F., Foit F.F. Jr., Wright, S.E., Brandstätter, F., and Marler, B. (2002) Polyhedron distortions in tourmaline. Canadian Mineralogist, 40, 153–162.

Ertl, A., Schuster, R., Prowatke, S., Brandstätter, F., Ludwig, T., Bernhardt, H.-J., Koller, F., and Hughes, J.M. (2004) Mn-rich tourmaline and fluorapatite in a Variscan pegmatite from Eibenstein an der Thaya, Bohemian massif, Lower Austria. European Journal of Mineralogy, 16, 551–560.

Ertl, A., Rossman, G.R., Hughes, J.M., Prowatke, S., and Ludwig, T. (2005) Mn-bearing "oxy-rossmanite" with tetrahedrally coordinated Al and B from Austria: Structure, chemistry, and infrared and optical spectroscopic study. American Mineralogist, 90, 481–487.

Ertl, A., Rossman, G.R., Hughes, J.M., London, D., Wang, Y., O'Leary, J.A., Dyar, M.D., Prowatke, S., Ludwig, T., and Tillmanns, E. (2010) Tourmaline of the elbaite-schorl series from the Himalaya Mine, Mesa Grande, California, U.S.A.: A detailed investigation. American Mineralogist, 95, 24–40.

Ertl, A., Schuster, R., Hughes, J.M., Ludwig, T., Meyer, H.-P., Finger, F., Dyar, M.D., Ruschel, K., Rossman, G.R., Klötzli, U., Brandstätter, F., Lengauer, C.L., and Tillmanns, E. (2012) Li-bearing tourmalines in Variscan pegmatites from the Moldanubian nappes, Lower Austria. European Journal of Mineralogy, 24, 695–715.

Fischer, R.X. and Tillmanns, E. (1988) The equivalent isotropic displacement factor. Acta Crystallographica, C44, 775–776.

Gadas P., Novák, M., Staněk, J., Filip, J., and Vašinová Galiová, M. (2012) Compositional evolution of zoned tourmaline crystals from pockets in common pegmatites, the Moldanubian Zone, Czech Republic. Canadian Mineralogist, 50, 895–912.

Henry, D., Novák, M., Hawthorne, F.C., Ertl, A., Dutrow, B., Uher, P., and Pezzotta, F. (2011) Nomenclature of the tourmaline-supergroup minerals. American Mineralogist, 96, 895–913.

London, D. (2011): Experimental synthesis and stability of tourmaline: a historical overview.

Canadian Mineralogist, 49, 117–136.

Lussier, A.J., Abdu, Y., Hawthorne, F.C., Michaelis, V.K., and Kroeker, S. (2011) Oscillatory zoned liddicoatite from Anjanabonoina, Central Madagascar I. Crystal chemistry and structure by SREF and ^{11}B and ^{27}Al MAS NMR spectroscopy. Canadian Mineralogist, 49, 63–88.

Melleton, J., Gloaguen, E., Frei, D., Novák, M., and Breiter, K. (2012) How are the time of emplacement of rare-element pegmatites, regional metamorphism and magmatism interrelated in the Moldanubian Domain of Variscan Bohemian Massif, Czech Republic? Canadian Mineralogist, 50, 1751–1773.

Merlet, C. (1994) An accurate computer correction program for quantitative electron probe micro-analysis. Mikrochimica Acta 114/115, 363–376.

Novák, M. (2000) Compositional pathways of tourmaline evolution during primary (magmatic) crystallization in complex (Li) pegmatites of the Moldanubicum, Czech Republic. Atti Societa Italiana di Scienze Naturale e Museo Civico di Storia Naturale Milano, 30, 45–56.

Novák, M. (2005) Granitic pegmatites of the Bohemian Massif (Czech Republic); mineralogical, geochemical and regional classification and geological significance. Acta Musei Moraviae, Scientiae Geologica, 90, 3–75. (in Czech with English summary)

Novák, M. and Černý, P. (1998) Niobium-tantalum oxide minerals from complex pegmatites in the Moldanubicum, Czech Republic; primary versus secondary compositional trends. Canadian Mineralogist, 36, 659–672.

Novák, M. and Povondra, P. (1995) Elbaite pegmatites in the Moldanubicum: a new subtype of the rare-element class. Mineralogy and Petrology, 55, 159–176.

Novák, M., Černý, P, Cooper M, Hawthorne F.C., Ottolini L., Xu Z., and Liang J-J. (1999b) Boron-bearing $2M_1$ polylithionite and $2M_1$ + 1M boromuscovite from an elbaite pegmatite at Řečice, western Moravia, Czech Republic. European Journal of Mineralogy, 11, 669–678.

Novák, M., Povondra, P., and Selway, J.B. (2004) Schorl-*oxy-schorl* to dravite-*oxy-dravite* tourmaline from granitic pegmatites; examples from the Moldanubicum, Czech Republic. European Journal of Mineralogy, 16, 323–333.

Novák, M., Selway, J.B., Černý, P., and Hawthorne, F.C. (1999a) Tourmaline of the elbaite-dravite series from an elbaite-subtype pegmatite at Bližná, southern Bohemia, Czech Republic. European Journal of Mineralogy, 11, 557–568.

Novák, M., Škoda, R., Filip, J., Macek, I., and Vaculovič, T. (2011) Compositional trends in tourmaline from the intragranitic NYF pegmatites of the Třebíč Pluton, Czech Republic; electron microprobe, LA-ICP-MS and Mössbauer study. Canadian Mineralogist, 49, 359–380.

Novák, M., Škoda, R., Gadas, P., Krmíček, L., and Černý, P. (2012) Contrasting origins of the mixed signature in granitic pegmatites; examples from the Moldanubian Zone, Czech Republic. Canadian Mineralogist Petr Černý Issue, 50, 1077–1094.

Peretti, A., Bieri, W.P., Reusser, E., Hametner, K., and Gunther, D. (2010) Chemical variations in multicolored "Paraiba"-type tourmalines from Brazil and Mozambique: implications for origin and authenticity determination. Contributions to Gemology, 9, 1-84.

Pezzotta, F. and Laurs B.M. (2011) Tourmaline: The Kaleidoscopic Gemstone. Elements, 7, 333–338.

Povondra, P., Čech, F., and Staněk, J. (1985) Crystal chemistry of elbaites from some pegmatites of the Czech Massif. Acta Universitatis Carolinae, Geologica, 1985, 1–24.

Reinitz, I.M. and Rossman, G.R. (1988) The role of natural radiation in tourmaline coloration. American Mineralogist, 73, 822–825.

Selway, J.B., Novák, M., Hawthorne, F.C., Černý, P., Ottolini, L., and Kyser, T.K. (1998) Rossmanite, $\square(LiAl_2)Al_6(Si_6O_{18})(BO_3)_3(OH)_4$, a new alkali-deficient tourmaline: description and crystal structure. American Mineralogist, 83, 896–900.

Selway, J.B., Novák, M., Černý, P., and Hawthorne, F.C. (1999) Compositional evolution of tourmaline in lepidolite-subtype pegmatites. European Journal of Mineralogy, 12, 569–584.

Selway, J.B., Černý, P., Hawthorne, F.C., and Novák, M. (2000) The Tanco pegmatite at Bernic Lake, Manitoba. XIV. Internal tourmaline. Canadian Mineralogist. 38, 1103–1117.

Selway, J.B., Smeds, S.-A., Černý, P., and Hawthorne, F.C. (2002) Compositional evolution of tourmaline in the petalite-subtype Nyköpingsgruvan pegmatites, Utö, Stockholm archipelago, Sweden. GFF, 124, 93–102.

Sheldrick, G.M. (1997) SHELXTL. Version 5.10. Bruker AXS Inc., Madison, Wisconsin, USA.

Smeds, S.A. and Černý, P. (1989) Pollucite from the Proterozoic petalite-bearing pegmatites of Uto, Stockholm archipelago, Sweden. GFF, 111, 361–372.

Stilling, A., Černý, P., and Vanstone, P.J. (2006) The Tanco pegmatite at Bernic Lake, Manitoba. XVI. Zonal and bulk compositions and their petrogenetic significance. Canadian Mineralogist, 44, 599–623.

Taran, M.N. and Rossman, G.R. (2001) Optical spectroscopic study of tuhualite and a re-examination of the beryl, cordierite, and osumilite spectra. American Mineralogist, 86, 973–980.

Teertstra, D.K., Černý, P., and Novák, M. (1995) Compositional and textural evolution of pollucite in rare-element pegmatites of the Moldanubicum. Mineralogy and Petrology, 55, 37–52.

Vernadsky, W. (1913) Über die chemische Formel der Turmaline. Zeitschrift für Kristallographie, Kristallogeometrie Kristallphysik, Kristallchemie, 53, 273–288.

Wise, A.M. and Brown, C.D. (2010) Mineral chemistry, petrology and geochemistry of the Sebago granite-pegmatite, southern Maine, USA. Journal of Geosciences, 55, 3–26.

Witter, J.B. and Kuehner, S.M. (2004) A simple empirical method for high-quality electron microprobe analysis of fluorine at trace levels in Fe-bearing minerals and glasses. American Mineralogist, 89, 57–63.

Zahradníček, L. and Novák, M. (2012) Lithium-bearing micas from elbaite-subtype pegmatites of Western Moravia, Czech Republic. Acta Musei Moraviae, Scientiae Geologicae, 97, 25–37. (in Czech with English summary)

Table 1. Theoretical compositions of olenite, along with known and hypothetical Li-bearing tourmalines.*

	1	2	3	4	5	6	7	8	9
SiO_2	39.03	38.65	38.49	38.40	38.12	38.12	38.2	37.84	37.41
Al_2O_3	44.15	46.46	40.82	40.73	43.12	37.73	37.81	40.13	47.61
B_2O_3	11.30	11.20	11.15	11.12	11.04	11.04	11.06	10.96	10.84
Li_2O	1.62	0.80	2.39	2.39	1.58	3.16	3.17	2.35	-
Na_2O	-	-	3.31	3.30	3.28	-	-	-	3.22
CaO	-	-	-	-	-	5.93	5.94	5.89	-
H_2O	3.90	2.90	3.85	2.88	2.86	2.86	3.82	2.84	0.93
F	-	-		2.02	-	2.01	-	-	-
X site	□	□	Na	Na	Na	Ca	Ca	Ca	Na
Y site	$LiAl_2$	$Li_{0.5}Al_{2.5}$	$Li_{1.5}Al_{1.5}$	$Li_{1.5}Al_{1.5}$	Li_1Al_2	Li_2Al_1	Li_2Al_1	$Li_{1.5}Al_{1.5}$	Al_3
Z site	Al_6	Al_6	Al_6	Al_6	Al_6	Al_6	Al_6	Al_6	Al_6
B site	B_3	B_3	B_3	B_3	B_3	B_3	B_3	B_3	B_3
T site	Si_6	Si_6	Si_6	Si_6	Si_6	Si_6	Si_6	Si_6	Si_6
V site	$(OH)_3$	$(OH)_3$	$(OH)_3$	$(OH)_3$	$(OH)_3$	$(OH)_3$	$(OH)_3$	$(OH)_3$	O_3
W site	OH	O	OH	F	O	F	OH	O	OH

*1: rossmanite □$(LiAl_2)Al_6Si_6O_{18}(BO_3)_3(OH)_3OH$; 2: □-Li-O root name □$(Li_{0.5}Al_{2.5})Al_6Si_6O_{18}(BO_3)_3(OH)_3O$; 3: elbaite $Na(Li_{1.5}Al_{1.5})Al_6Si_6O_{18}(BO_3)_3(OH)_3OH$; 4: fluor-elbaite $Na(Li_{1.5}Al_{1.5})Al_6Si_6O_{18}(BO_3)_3(OH)_3F$; 5: darrellhenryite $Na(LiAl_2)Al_6Si_6O_{18}(BO_3)_3(OH)_3O$; 6: fluor-liddicoatite $Ca(Li_2Al)Al_6Si_6O_{18}(BO_3)_3(OH)_3F$; 7: *liddicoatite* $Ca(Li_2Al)Al_6Si_6O_{18}(BO_3)_3(OH)_3OH$; 8: Ca-Li-O root name $Ca(Li_{1.5}Al_{1.5})Al_6Si_6O_{18}(BO_3)_3(OH)_3O$; 9: olenite $NaAl_3Al_6Si_6O_{18}(BO_3)_3(O)_3OH$; all formulas from Henry et al. (2011)

482 Table 2. Analytical data for darrellhenryite.

Constituent	wt%[a]	wt%[b]	Range[b]	SD[b]	Probe Standard
SiO_2	37.94	38.38	38.69-38.12	0.17	almandine
Al_2O_3	42.77	43.49	43.75-43.10	0.16	grossular
B_2O_3	11.01	11.01[a]			
FeO	0.17				almandine
MnO	0.02	0.02	0.11-0.00	0.04	spessartine
CaO	0.07	0.05	0.09-0.00	0.03	fluorapatite
Li_2O	1.88	1.63	1.87-1.37	0.21	NIST 610
Na_2O	1.81	1.92	2.03-1.78	0.07	albite
K_2O	0.12				sanidine
H_2O	2.86	2.86[a]			
F	0.64	0.71	0.78-0.61	0.07	*lepidolite*
O = F	-0.27	-0.30			
Total	99.02	99.77			

483 [a]Wet chemical analysis from Povondra et al. (1985). [b]Electron microprobe, LA-ICP-MS
484 (Li_2O), TGA: 2.9(1) wt% H_2O, near-infrared spectroscopy: 2.87 wt% H_2O.
485
486

Table 3: Crystallographic data and refinement details for darrellhenryite.

a, *c* (Å)	15.809(2), 7.089(1)
V (Å^3)	1534.4(7)
Crystal dimensions (mm)	0.15 x 0.15 x 0.10
Collection mode, $2\theta_{max}$ (°)	full sphere, 79.95
h, k, l ranges	-28/28, -28/27, -12/12
Number of frames	620
Total reflections measured	19944
Unique reflections	2249
$R1^*(F)$, $wR2^{\dagger}(F^2)$, $R_{int}^{\ddagger}$ (%)	1.95%, 4.32%, 3.50%
Flack *x* parameter	0.016(59)
'Observed' refls. [$F_o > 4\sigma_{(Fo)}$]	2169
Extinct. Coefficient	0.00517(26)
No. of refined parameters	95
Goodness-of-Fit§	1.065
$\Delta\sigma_{min}$, $\Delta\sigma_{max}$ (e/Å^3)	-0.57, 0.64

Note: X-ray radiation: Mo*K*α (λ = 0.71073 Å); *Z*: 3; space group: *R*3*m* (no. 160); multi-scan absorption correction; refinement on F^2. Frame width, scan time, detector distance: 3°, 15 s, 35 mm. Scan mode: sets of ϖ and θ scans.

* $R1 = \Sigma| |F_o| - |F_c| | / \Sigma|F_o|$

† $wR2 = \{\Sigma[w(F_o^2 - F_c^2)^2] / \Sigma[w(F_o^2)^2]\}^{1/2}$

$w = 1 / [\sigma^2(F_o^2) + (aP)^2 + bP]$, $P = [2F_c^2 + \mathrm{Max}(F_o^2,0)] / 3$

‡ $R_{int} = \Sigma|F_o^2 - F_o^2(\mathrm{mean})| / \Sigma[F_o^2]$

§ $\mathrm{GooF} = S = \{\Sigma[w(F_o^2 - F_c^2)^2] / (n-p)\}^{1/2}$

499 Table 4: Table of atomic parameters in darrellhenryite.

Site	***x***	***y***	***z***	U_{eq}	***Occ.***
X	0	0	0.7509(3)	0.0199(6)	$Na_{0.56(1)}$
Y	0.87800(4)	0.93900(2)	0.34846(7)	0.0068(2)	$Al_{0.651(3)}Li_{0.349}$
Z	0.70347(2)	0.74017(2)	0.37588(3)	0.00539(5)	$A_{1.00}$
B	0.89096(4)	0.78193(9)	0.5307(2)	0.0057(2)	$B_{1.00}$
T	0.80823(1)	0.81027(2)	0.98406(3)	0.00450(4)	$Si_{1.00}$
H3	0.740(2)	0.870(1)	0.600(4)	0.051(8)	$H_{1.00}$
O1	0	0	0.2079(2)	0.0252(6)	$O_{0.66(4)}F_{0.34}$
O2	0.93962(3)	0.87924(7)	0.4938(1)	0.0125(2)	$O_{1.00}$
O3	0.73727(8)	0.86864(4)	0.4772(1)	0.0124(2)	$O_{1.00}$
O4	0.90589(3)	0.81179(7)	0.9106(1)	0.0085(1)	$O_{1.00}$
O5	0.81242(7)	0.90621(4)	0.8883(1)	0.0091(1)	$O_{1.00}$
O6	0.80533(4)	0.81595(4)	0.21009(8)	0.0070(1)	$O_{1.00}$
O7	0.71341(4)	0.71375(4)	0.90703(7)	0.00641(9)	$O_{1.00}$
O8	0.79052(4)	0.72987(4)	0.54631(8)	0.0071(1)	$O_{1.00}$

500

501 Note: For the definition of U_{eq} see Fischer and Tillmanns (1988).

502

503 Table 5: Selected interatomic distances in darrellhenryite.

504

X-	
O2 x3	2.461(2)
O5 x3	2.747(1)
O4 x3	2.815(1)
Mean	2.674(1)
Y-	
O1	1.9450(11)
O2 x2	1.9552(7)
O6 x2	1.9574(7)
O3	2.1320(12)
Mean	1.9837(9)
Z-	
O6	1.8656(6)
O7	1.8815(6)
O8	1.8850(6)
O8’	1.8985(7)
O7’	1.9425(6)
O3	1.9598(5)
Mean	1.9055(6)
T-	
O7	1.6069(7)
O6	1.6081(6)
O4	1.6180(4)
O5	1.6326(4)
Mean	1.6164(5)
B-	
O2	1.358(2)
O8 (x2)	1.3799(9)
Mean	1.373(1)

505

506 Standard deviation in brackets.

507

508 Table 6. X-ray powder diffraction data for darrellhenryite.
509

d_{meas} (Å)	d_{calc} (Å)	I_{meas}	h	k	l
7.906	7.911	5	1	1	0
6.295	6.299	15	1	0	1
4.924	4.927	18	0	2	1
4.575	4.578	7	3	0	0
4.180	4.183	**39**	2	1	1
3.952	3.954	**54**	2	2	0
3.431	3.434	**73**	0	1	2
3.353	3.355	18	1	3	1
3.084	3.086	8	4	0	1
2.989	2.991	14	4	1	0
2.925	2.927	**100**	1	2	2
2.873	2.875	4	3	2	1
2.592	2.594	11	3	1	2
2.555	2.557	**90**	0	5	1
2.433	2.435	1	2	4	1
2.364	2.366	38	0	0	3
2.355	2.356	31	2	3	2
2.326	2.328	**42**	5	1	1
2.284	2.286	3	6	0	0
2.266	2.267	2	1	1	3
2.168	2.170	13	5	0	2
2.147	2.148	21	4	3	1
2.100	2.101	25	3	0	3
2.090	2.091	14	4	2	2
2.029	2.030	**42**	2	2	3
2.021	2.023	**42**	1	5	2
2.004	2.005	10	1	6	1
1.978	1.979	4	4	4	0
1.901	1.902	**50**	3	4	2
1.887	1.888	6	3	5	1
1.854	1.855	12	4	1	3
1.835	1.837	9	6	2	1
1.816	1.817	3	7	1	0
1.802	1.803	1	6	1	2
1.759	1.760	15	1	0	4
1.718	1.719	5	0	2	4
1.674	1.675	6	2	6	2
1.643	1.644	**49**	6	0	3
1.629	1.630	27	2	7	1
1.608	1.609	2	5	2	3
1.582	1.583	20	5	5	0
1.576	1.577	9	4	0	4
1.565	1.566	4	8	1	1
1.544	1.545	6	3	2	4
1.534	1.535	8	4	6	1

1.523	1.524	9	9	0	0
1.514	1.515	11	7	2	2
1.508	1.508	3	7	3	1

Note: *d*-values in Å. The unit-cell data parameters refined from the powder data (Cu*K*α radiation) are $a = 15.820(2)$, $c = 7.093(1)$ Å.

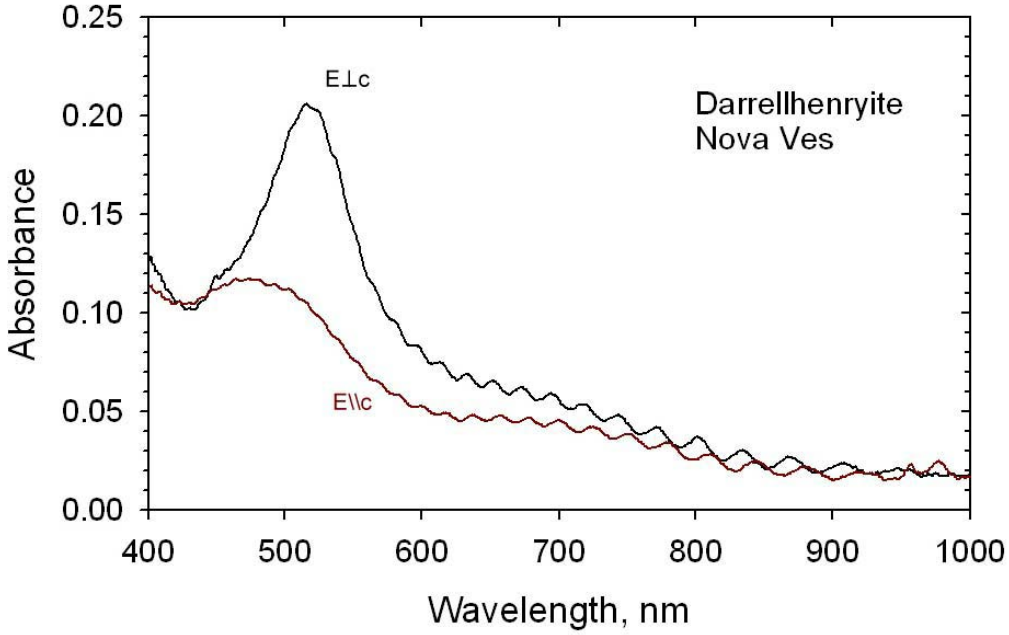

514

515 Figure 1. Optical absorption spectrum of darrellhenyrite normalized to 1.0 mm
516 thickness.

517

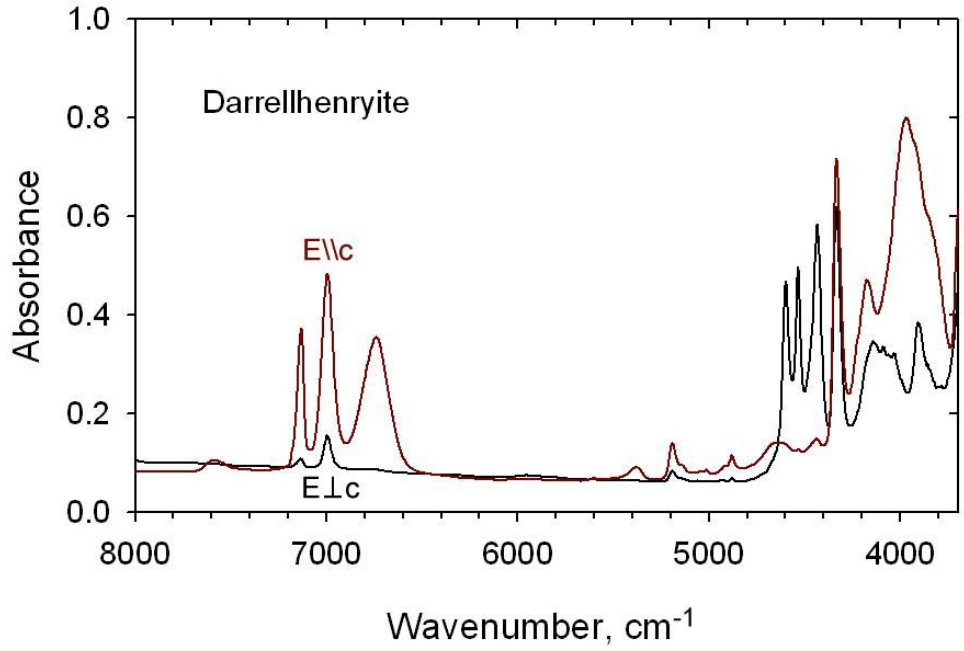

518

519 Figure 2. Near-IR spectrum of darrellhenryite (sample grr3075).

520

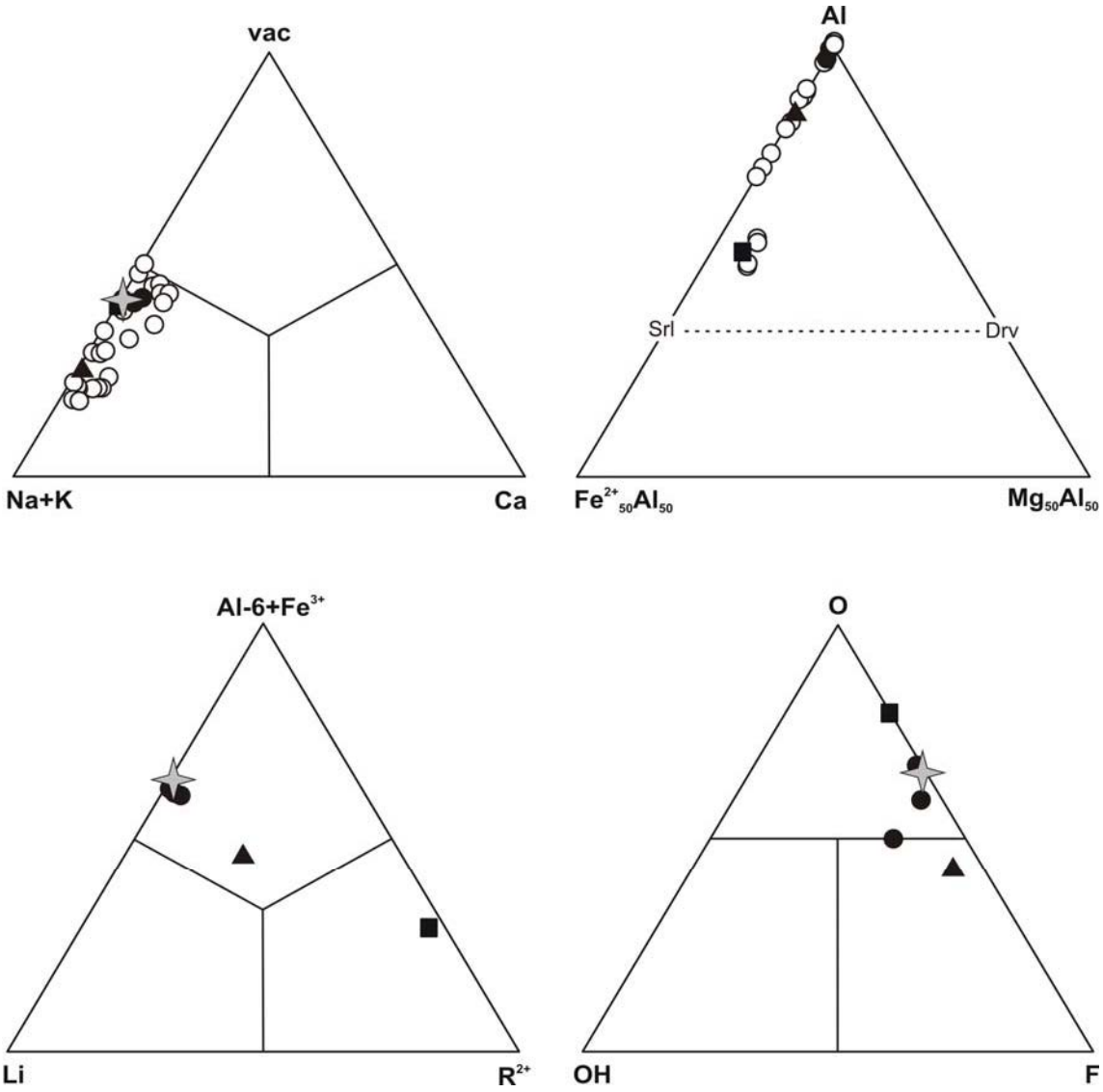

521

522

523 Figure. 3. Chemical composition of tourmalines from the Nová Ves pegmatite. Open circles -
524 EMPA data; solid symbols - wet chemical analyses (Povondra et al. 1985): square -black oxy-
525 schorl, triangle - green Fe-rich fluor-elbaite, circles - pink darrellhenryite to darrellhenryite -
526 fluor-elbaite; star - type material data (Table 2, analysis b).

This is a preprint, the final version is subject to change, of the American Mineralogist (MSA)
Cite as Authors (Year) Title. American Mineralogist, in press.
(DOI will not work until issue is live.) DOI: http://dx.doi.org/10.2138/am.2013.4416

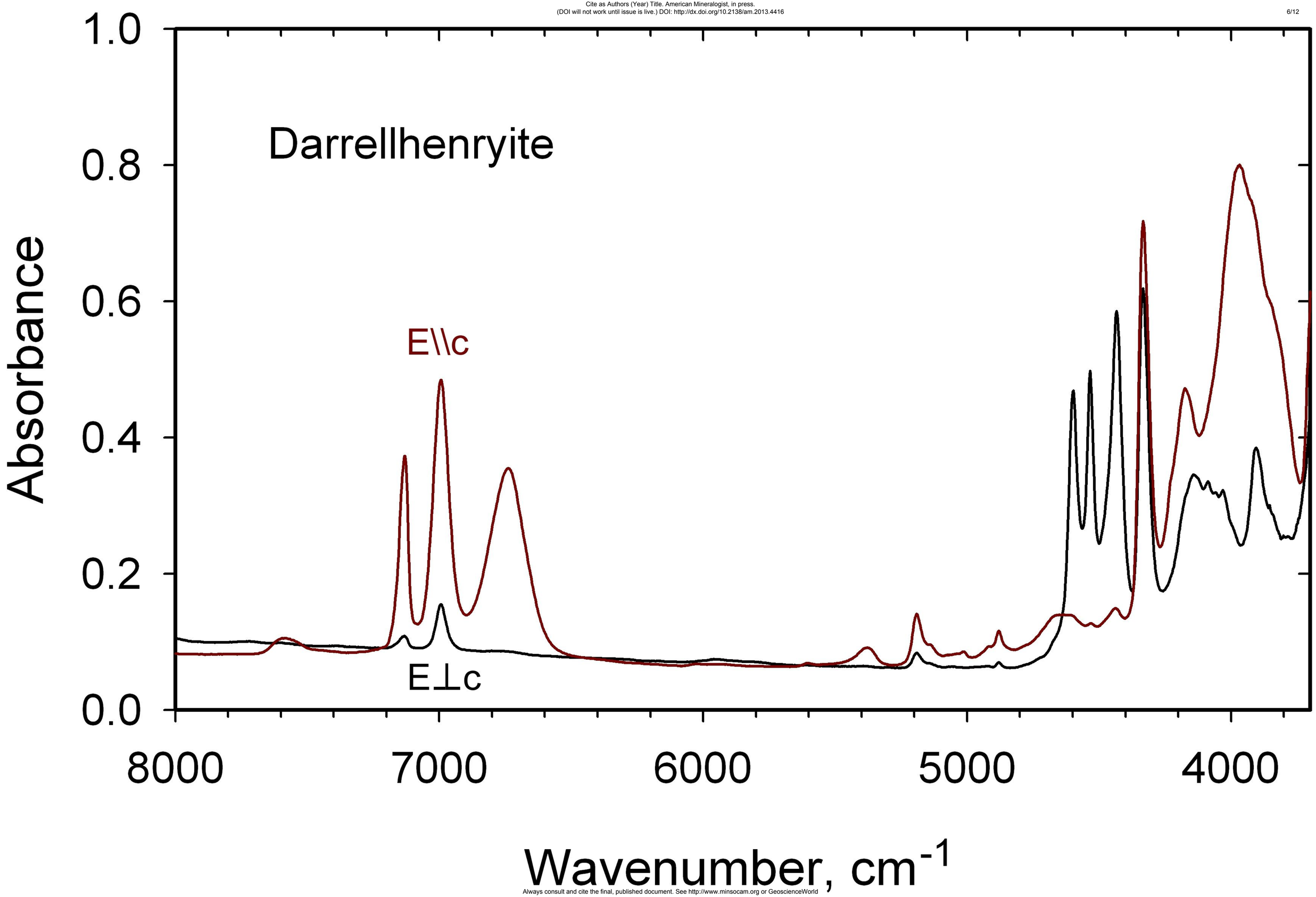

This is a preprint, the final version is subject to change, of the American Mineralogist (MSA)
Cite as Authors (Year) Title. American Mineralogist, in press.
(DOI will not work until issue is live.) DOI: http://dx.doi.org/10.2138/am.2013.4416

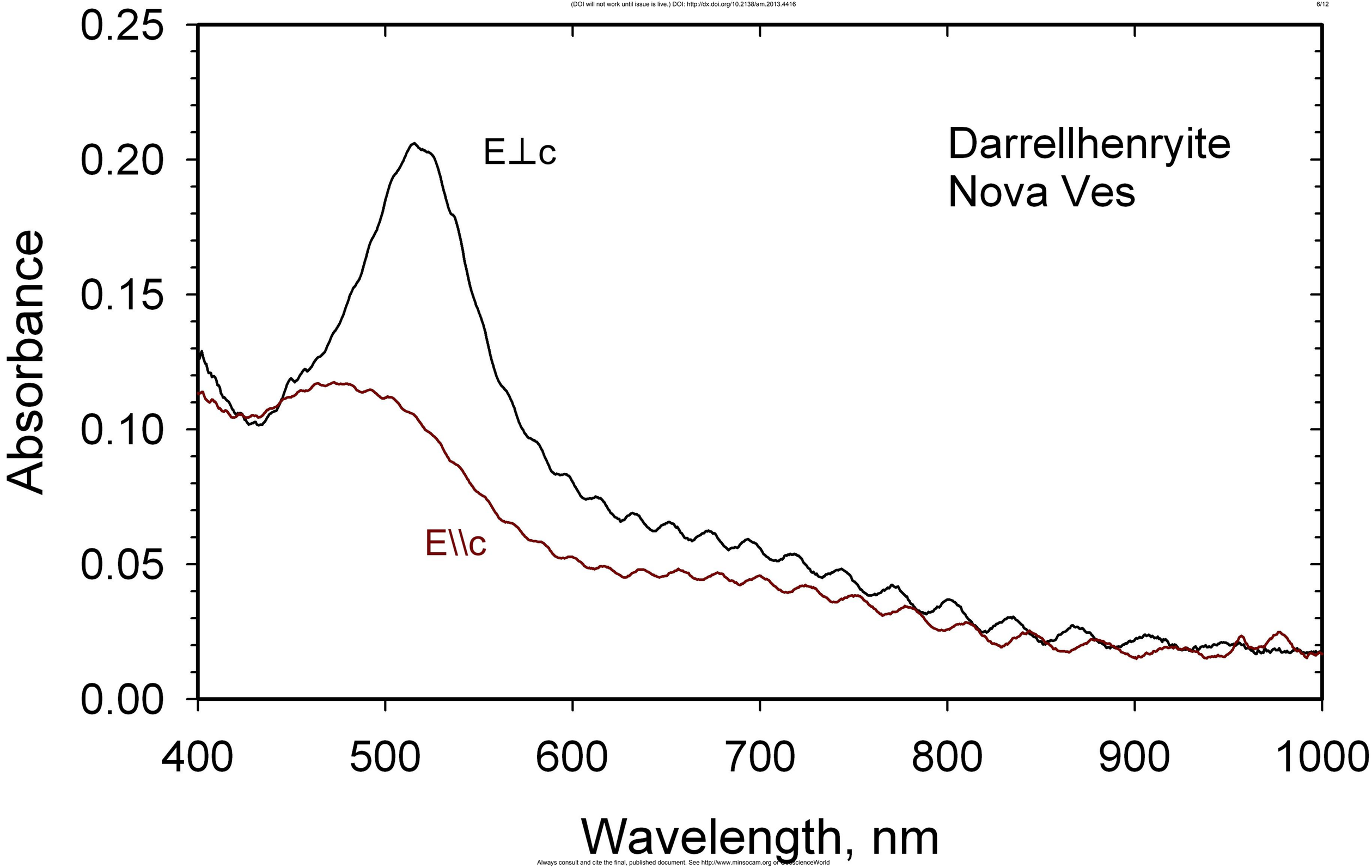

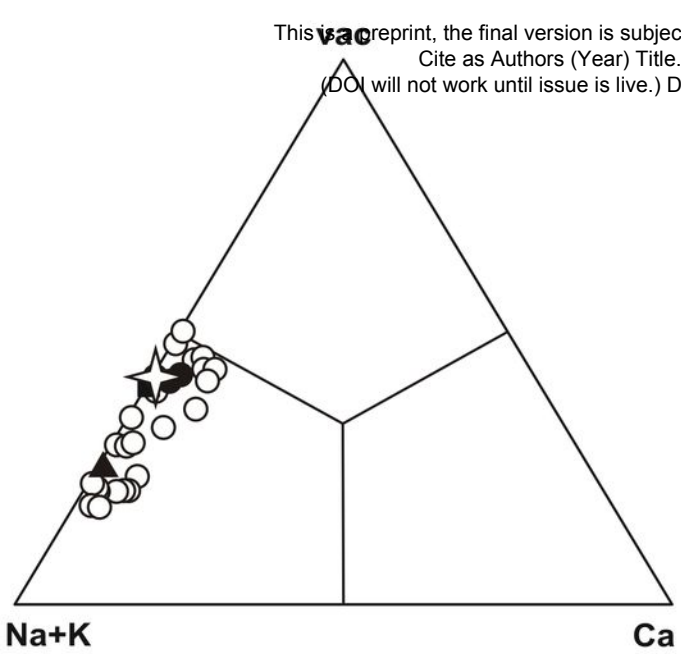

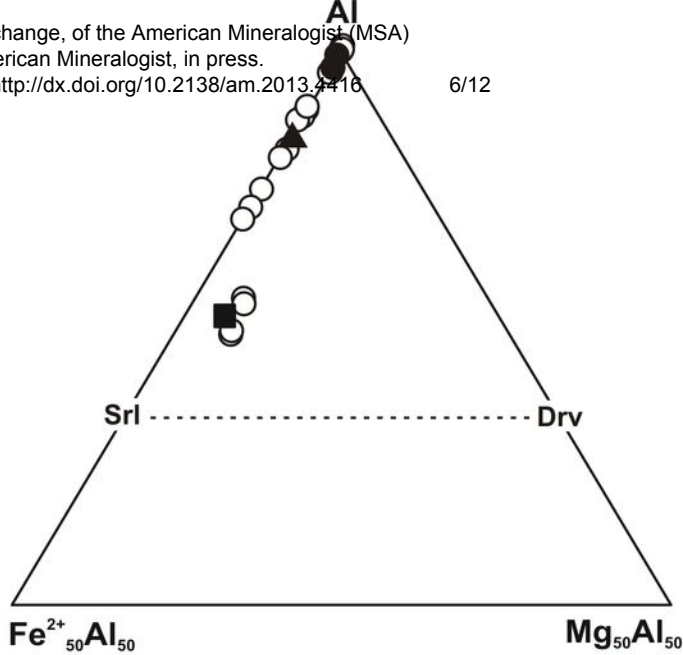

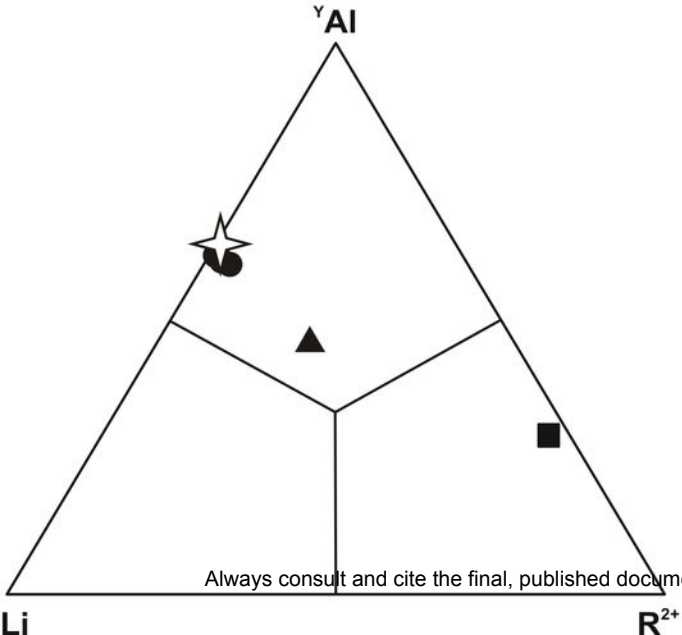

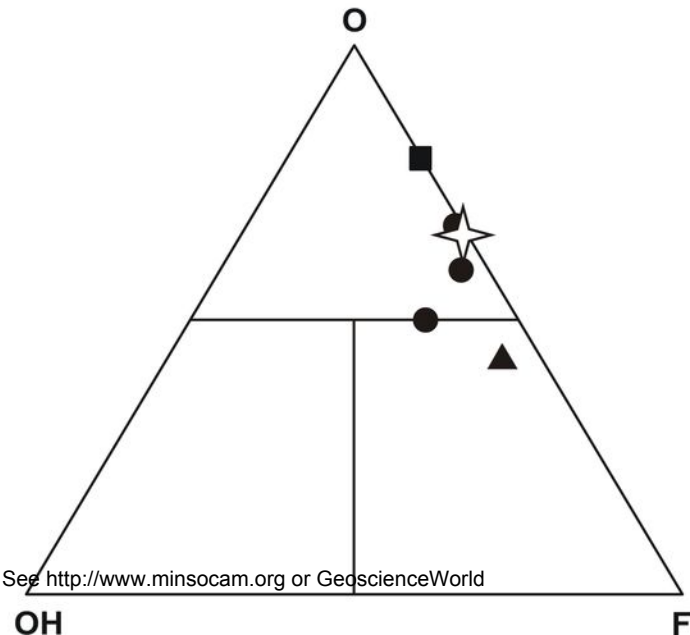

	1	2	3	4	5	6	7	8	9
SiO_2	39.03	38.65	38.49	38.40	38.12	38.12	38.20	37.84	37.41
Al_2O_3	44.15	46.46	40.82	40.73	43.12	37.73	37.81	40.13	47.61
B_2O_3	11.30	11.20	11.15	11.12	11.04	11.04	11.06	10.96	10.84
Li_2O	1.62	0.80	2.39	2.39	1.58	3.16	3.17	2.35	-
Na_2O	-	-	3.31	3.30	3.28	-	-	-	3.22
CaO	-	-	-	-	-	5.93	5.94	5.89	-
H_2O	3.90	2.90	3.85	2.88	2.86	2.86	3.82	2.84	0.93
F	-	-		2.02	-	2.01	-	-	-
X site	□	□	Na	Na	Na	Ca	Ca	Ca	Na
Y site	$LiAl_2$	$Li_{0.5}Al_{2.5}$	$Li_{1.5}Al_{1.5}$	$Li_{1.5}Al_{1.5}$	Li_1Al_2	Li_2Al_1	Li_2Al_1	$Li_{1.5}Al_{1.5}$	Al_3
Z site	Al_6	Al_6	Al_6	Al_6	Al_6	Al_6	Al_6	Al_6	Al_6
B site	B_3	B_3	B_3	B_3	B_3	B_3	B_3	B_3	B_3
T site	Si_6	Si_6	Si_6	Si_6	Si_6	Si_6	Si_6	Si_6	Si_6
V site	$(OH)_3$	$(OH)_3$	$(OH)_3$	$(OH)_3$	$(OH)_3$	$(OH)_3$	$(OH)_3$	$(OH)_3$	O_3
W site	OH	O	OH	F	O	F	OH	O	OH

Constituent	wt%[a]	wt%[b]	Range[b]	SD[b]	Probe Standard
SiO_2	37.94	38.38	38.69-38.12	0.17	almandine
Al_2O_3	42.77	43.49	43.75-43.10	0.16	grossular
B_2O_3	11-Jan	11.01[a]			
FeO	0.17				almandine
MnO	0.02	0.02	0.11-0.00	0.04	spessartine
CaO	0.07	0.05	0.09-0.00	0.03	fluorapatite
Li_2O	Jan-88	Jan-63	1.87-1.37	0.21	NIST 610
Na_2O	Jan-81	Jan-92	2.03-1.78	0.07	albite
K_2O	0.12				sanidine
H_2O	Feb-86	2.86[a]			
F	0.64	0.71	0.78-0.61	0.07	*lepidolite*
O = F	-0.27	-0.30			
Total	99.02	99.77			

a, c (Å)	15.809(2), 7.089(1)
V (Å^3)	1534.4(7)
Crystal dimensions (mm)	0.15 x 0.15 x 0.10
Collection mode, $2\theta_{max}$ (°)	full sphere, 79.95
h, k, l ranges	-28/28, -28/27, -12/12
Number of frames	620
Total reflections measured	19944
Unique reflections	2249
R 1*(F), wR 2†(F^2), R_{int} ‡ (%)	1.95%, 4.32%, 3.50%
Flack x parameter	0.016(59)
'Observed' refls. [$F_o > 4\sigma_{(F o)}$]	2169
Extinct. Coefficient	0.00517(26)
No. of refined parameters	95
Goodness-of-Fit§	1.065
$\Delta\sigma_{min}$, $\Delta\sigma_{max}$ (e/Å^3)	-0.57, 0.64

Site	*x*	*y*	*z*	U_{eq}	*Occ.*
X	0	0	0.7509(3)	0.0199(6)	$Na_{0.56(1)}$
Y	0.87800(4)	1/2x	0.34846(7)	0.0068(2)	$Al_{0.651(3)}Li_{0.349}$
Z	0.70347(2)	0.74017(2)	0.37588(3)	0.00539(5)	$A_{1.00}$
B	0.89096(4)	2x	0.5307(2)	0.0057(2)	$B_{1.00}$
T	0.80823(1)	0.81027(2)	0.98406(3)	0.00450(4)	$Si_{1.00}$
H3	0.740(2)	1/2x	0.600(4)	0.051(8)	$H_{1.00}$
O1	0	0	0.2079(2)	0.0252(6)	$O_{0.66(4)}F_{0.34}$
O2	0.93962(3)	2x	0.4938(1)	0.0125(2)	$O_{1.00}$
O3	0.73727(8)	1/2x	0.4772(1)	0.0124(2)	$O_{1.00}$
O4	0.90589(3)	2x	0.9106(1)	0.0085(1)	$O_{1.00}$
O5	0.81242(7)	1/2x	0.8883(1)	0.0091(1)	$O_{1.00}$
O6	0.80533(4)	0.81595(4)	0.21009(8)	0.0070(1)	$O_{1.00}$
O7	0.71341(4)	0.71375(4)	0.90703(7)	0.00641(9)	$O_{1.00}$
O8	0.79052(4)	0.72987(4)	0.54631(8)	0.0071(1)	$O_{1.00}$

X -	
O2 x3	2.461(2)
O5 x3	2.747(1)
O4 x3	2.815(1)
Mean	2.674(1)
Y -	
O1	1.9450(11)
O2 x2	1.9552(7)
O6 x2	1.9574(7)
O3	2.1320(12)
Mean	1.9837(9)
Z -	
O6	1.8656(6)
O7	1.8815(6)
O8	1.8850(6)
O8’	1.8985(7)
O7’	1.9425(6)
O3	1.9598(5)
Mean	1.9055(6)
T -	
O7	1.6069(7)
O6	1.6081(6)
O4	1.6180(4)
O5	1.6326(4)
Mean	1.6164(5)

B-	
O2	1.358(2)
O8 (x2)	1.3799(9)
Mean	1.373(1)

d_{meas} (Å)	d_{calc} (Å)	I_{meas}	h	k	l
7.906	7.911	5	1	1	0
6.295	6.299	15	1	0	1
4.924	4.927	18	0	2	1
4.575	4.578	7	3	0	0
4.180	4.183	**39**	2	1	1
3.952	3.954	**54**	2	2	0
3.431	3.434	**73**	0	1	2
3.353	3.355	18	1	3	1
3.084	3.086	8	4	0	1
2.989	2.991	14	4	1	0
2.925	2.927	**100**	1	2	2
2.873	2.875	4	3	2	1
2.592	2.594	11	3	1	2
2.555	2.557	**90**	0	5	1
2.433	2.435	1	2	4	1
2.364	2.366	38	0	0	3
2.355	2.356	31	2	3	2
2.326	2.328	**42**	5	1	1
2.284	2.286	3	6	0	0
2.266	2.267	2	1	1	3
2.168	2.170	13	5	0	2
2.147	2.148	21	4	3	1
2.100	2.101	25	3	0	3
2.090	2.091	14	4	2	2
2.029	2.030	**42**	2	2	3
2.021	2.023	**42**	1	5	2
2.004	2.005	10	1	6	1
1.978	1.979	4	4	4	0

1.901	1.902	**50**	3	4	2
1.887	1.888	6	3	5	1
1.854	1.855	12	4	1	3
1.835	1.837	9	6	2	1
1.816	1.817	3	7	1	0
1.802	1.803	1	6	1	2
1.759	1.760	15	1	0	4
1.718	1.719	5	0	2	4
1.674	1.675	6	2	6	2
1.643	1.644	**49**	6	0	3
1.629	1.630	27	2	7	1
1.608	1.609	2	5	2	3
1.582	1.583	20	5	5	0
1.576	1.577	9	4	0	4
1.565	1.566	4	8	1	1
1.544	1.545	6	3	2	4
1.534	1.535	8	4	6	1
1.523	1.524	9	9	0	0
1.514	1.515	11	7	2	2
1.508	1.508	3	7	3	1